International Journal of Thermophysics (2022) 43:2
https://doi.org/10.1007/s10765-021-02926-6

Uncertainty Assessment for Very High Temperature Thermal Diffusivity Measurements on Molybdenum, Tungsten and Isotropic Graphite

Bruno Hay[1] · Olivier Beaumont[1] · Guillaume Failleau[1] · Nolwenn Fleurence[1] · Marc Grelard[1] · Refat Razouk[1] · Guillaume Davée[1] · Jacques Hameury[1]

Received: 11 September 2021 / Accepted: 30 September 2021 / Published online: 17 October 2021

Abstract
The French National Metrology Institute LNE has improved its homemade laser flash apparatus in order to perform accurate and reliable measurements of thermal diffusivity of homogeneous solid materials at very high temperature. The inductive furnace and the associated infrared (IR) detection systems have been modified and a specific procedure for the *in situ* calibration of the used radiation thermometers has been developed. This new configuration of the LNE's diffusivimeter has been then applied for measuring the thermal diffusivity of molybdenum up to 2200 °C, tungsten up to 2400 °C and isotropic graphite up to 3000 °C. Uncertainties associated with these high temperature thermal diffusivity measurements have been assessed for the first time according to the principles of the "Guide to the Expression of Uncertainty in Measurement" (GUM). Detailed uncertainty budgets are here presented in the case of the isotropic graphite for measurements performed at 1000 °C, 2000 °C and 3000 °C. The relative expanded uncertainty (coverage factor $k=2$) of the thermal diffusivity measurement is estimated to be between 3 % and 5 % in the whole temperature range for the three investigated refractory materials.

Keywords High temperature · Isotropic graphite · Molybdenum · Thermal diffusivity · Tungsten · Uncertainty

1 Introduction

Nuclear energy and space industries, which operate facilities and equipment at temperatures above 1500 °C, have used for a long time high temperature resistant materials for their specific applications [1, 2]. Thanks to emerging developments

✉ Bruno Hay
bruno.hay@lne.fr

[1] Laboratoire National de Métrologie et d'Essais, Laboratoire Commun de Métrologie (LNE-CNAM), 29 avenue Roger Hennequin, 78197 Trappes, France

in material science, these industries develop new refractory materials able to work at higher temperatures in order to optimise their processes and to expand safety margins and the efficiency of particular technologies.

In nuclear applications, silicon carbide-based composite materials are seen today as a promising alternative to the current zirconium-based alloys (commonly used for manufacturing fuel claddings) for the use of accident tolerant fuel as their oxidation temperature is far higher than that of zirconium-based alloys (approximately 2000 °C *versus* 1200 °C) [3, 4]. In space applications, space modules and vehicles [5, 7] need thermal shields for their exploratory missions or during re-entry in atmosphere in order to resist to temperatures that can be higher than 2500 °C.

In the examples above, the knowledge of the thermal diffusivity of the used advanced materials as a function of temperature is crucial for predicting their behaviour in real conditions. In addition, accurate data of thermal diffusivity are also needed for the thermal modelling of abnormal and accident scenarios, during which materials would be exposed to ultra-high temperatures.

Although some dedicated facilities exist in the concerned industries for measuring thermal diffusivity, it is not possible to ensure the reliability of the measured data above 1500 °C and their traceability to the International System of Units (SI), due to a lack of appropriate standard reference materials and reference facilities.

To address these metrological needs, LNE has improved the measurement capabilities of its reference apparatus based on the laser flash method to measure thermal diffusivity of homogeneous solid materials up to 3000 °C with a target expanded uncertainty of few percent. This work has been performed within the framework of the European joint research project "Hi-TRACE—Industrial process optimisation through improved metrology of thermophysical properties" [8]. The overall objective of the Hi-TRACE project, coordinated by LNE, is to establish a European metrological infrastructure composed of reference facilities in order to provide industries with traceable thermophysical properties measurements (thermal diffusivity, specific heat and emissivity) at very high temperature.

Several papers dealing with uncertainty analysis associated with thermal diffusivity measurements performed using the laser flash method have been published during the last two decades. They present the identification and quantification of influencing parameters and sources of measurement errors [9, 10], the establishment of detailed uncertainty budgets [11, 12] according to the ISO/BIPM Guide to the expression of uncertainty in measurement [13], or the development of alternative approaches (*e.g.*, Bayesian or multi-convolutional approaches) to evaluate the uncertainty on thermal diffusivity measurements [14–16]. All these published works are limited to measurements performed from room temperature to 1000 °C at maximum, and sometimes do not take into account the contribution of some significant uncertainty factors (spatially non-uniform heating, non-linearity of the infrared detector output with respect to temperature, variation of the specimen thickness due to the thermal expansion of the tested material…).

After a brief description of the metrological facility and method that have been implemented at LNE for measuring the thermal diffusivity up to 3000 °C, this paper presents the results obtained on isotropic graphite, tungsten and molybdenum

specimens, and for the first time gives detail of uncertainty budgets associated with very high temperature thermal diffusivity measurements.

2 Method of Measurement

LNE has performed for many years thermal diffusivity measurements of homogeneous solid materials up to 2000 °C in inert or vacuum environments by using a homemade facility [17] based on the well-known principle of the *rear face* laser flash method [18]. In this method, a cylindrical specimen is heated on its front face by a short energy pulse, and the induced transient temperature rise is measured on its back face *versus* time. The thermal diffusivity is determined with an estimation procedure based on minimizing the difference between the experimental temperature–time curve (thermogram) and the same curve given by a theoretical model of the transient heat conduction through the specimen. In the case of a bulk homogeneous material, the thermal diffusivity is estimated by LNE according to the *partial time moments method* [19]. This identification method was used by LNE for example in the certification process of Pyroceram 9606 as BCR-724 reference material [20] and in the first international inter-laboratory comparison on thermal diffusivity measurements organized by the Bureau International des Poids et Mesures (BIPM) [21, 22].

2.1 Description of the Apparatus

In its former configuration, the laser flash apparatus of LNE was equipped with two furnaces, a resistive furnace operating from room temperature to 800 °C and an inductive one for the measurements performed from 700 °C to 2000 °C. The inductive furnace has been recently improved to enable the thermal diffusivity measurement of solid homogeneous materials up to 3000 °C.

A schematic representation of this facility is shown in Fig. 1a. The specimen (disk of 10 mm in diameter and 1 mm to 4 mm thick) is maintained at a constant temperature in the inductive furnace composed by an airtight enclosure water cooled in the centre of which an inductive coil and a movable susceptor are placed on a vertical axis.

The inductive coil is a copper solenoid also cooled by circulation of water and connected to a 50 kW high frequency generator (100 kHz to 400 kHz). Its geometry has been optimised (reduction of the number of turns from 5 to 4 to increase the distance between each turn and coating of the coil with a ceramic deposit) in order to avoid the appearance of sparks between the susceptor and the coil as well as sparks between the turns themselves that can damage the susceptor and disturb the measurements. Figure 1b presents a picture of the new copper induction coil with the ceramic coating.

The susceptor is a hollow cylinder having a shoulder machined at mid-height to maintain the specimen. The Foucault currents induced in the susceptor generate heat by Joule heating, the specimen located inside being then heated primarily by

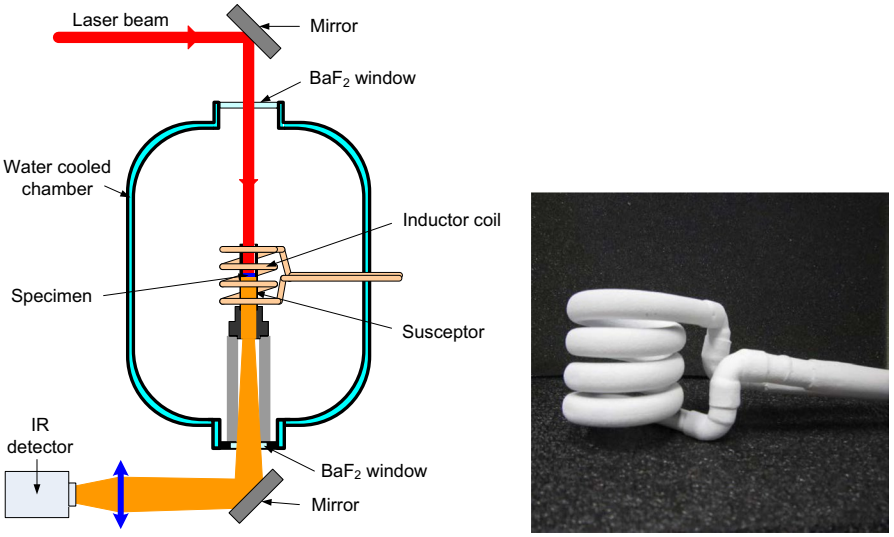

(a) *Schematic diagram of the diffusivimeter of LNE* **(b)** *Inductive coil*

Fig. 1 LNE facility for the thermal diffusivity measurement of solid materials up to 3000 °C

radiative transfer. Depending on the temperature range and the material of the specimen, a thin washer made of molybdenum or tungsten is put between the specimen and the graphite susceptor in order to avoid any direct contact between them with the objective to limit chemical interactions at high temperature. The geometry of the susceptor has been modified and the diameter of its support has been reduced in order to limit conduction heat losses. The cooling loop of the inductive coil and of the enclosure has been improved in order to both increase the cooling efficiency and to reduce the temperature variations of the enclosure wall from 29 °C ± 2 °C to 29 °C ± 0.3 °C.

Two power supplies have been implemented in the high frequency generator of the inductive furnace in order to optimize the temperature resolution depending on the level of temperature: a 25 kW configuration enabling to reach 2800 °C with a temperature resolution of 12 °C at 1000 °C and 1 °C at 2800 °C, and a 50 kW configuration for higher temperatures with temperature resolution of 25 °C at 1000 °C and 2 °C at 3000 °C. A filter has been put at the output of the HF generator to reduce the high frequency electromagnetic interferences (> 250 kHz). These modifications enable to increase the signal to noise ratio and therefore to obtain exploitable thermograms up to 3000 °C. The furnace is equipped with two BaF_2 windows, which are transparent (transmission higher than 90 % from 0.25 µm up to 10 µm) to the laser wavelength and to the wavelength ranges of the IR detectors.

The temperature of the specimen is measured during heating of the furnace as well as when temperature is stabilized at target temperature with one of the two infrared bi-chromatic radiation thermometers (0.90 µm and 1.05 µm) operating in the temperature ranges [700 °C to 1800 °C] or [1000 °C to 3000°]. They are installed on a linear stage enabling to put one or the other opposite the 90°

flat mirror attached below the movable susceptor. These radiation thermometers can be subjected to drift along time and need thus to be periodically calibrated to ensure trueness of temperature measurements. A specific protocol, based on the use of metal–carbon eutectic high temperature fixed points positioned in the furnace at the location of the specimens, has been therefore developed at LNE in order to enable the *in situ* calibration of the radiation thermometers [23]. The eutectic fixed points are palladium-carbon (1492 °C), platinum–carbon (1738 °C) and iridium-carbon (2290 °C).

The short thermal excitation (duration around 450 µs) is generated by a Nd:phosphate glass laser at 1054 nm wavelength, whose beam is formed by a set of lenses, mirrors and stops so that its diameter is about 10 mm on the front face of the specimen. A photodiode is used to measure the duration, the temporal profil of the pulse, and the time origin that corresponds to the time when the laser beam irradiates the specimen. The induced transient temperature rise of the specimen rear face is measured optically with an infrared detector (HgCdTe, InGaAs and Si depending on the temperature range). An optical system made of lenses is associated to each IR detector in order to collect the infrared radiation emitted by the specimen rear face.

2.2 Estimation Process of Thermal Diffusivity

The thermal diffusivity is determined by identification of the experimental thermogram with a theoretical model, which is in the classical case of a homogeneous material a two-parameter unidirectional model depending on the thermal diffusivity a and the dimensionless Biot number Bi (which represents the thermal exchanges between the specimen and its surrounding). This analytical model is obtained by solving the heat conduction equation for the case of a homogeneous, isotropic and opaque specimen assuming that the model is linear (thermophysical properties are considered independent of the temperature), the heat losses between the sample and its surrounding are characterized by a uniform and constant in time heat exchange coefficient, the laser pulse is spatially uniform and can be considered as a Dirac pulse.

In the *partial time moments method* [19], the thermal diffusivity is estimated from the partial time moments of order 0 and -1 determined for the experimental and theoretical thermograms *f(t)* normalized by their *maxima* (an example of experimental thermogram is given in Fig. 2).

$$f(t) = (U(t) - U_0)/(U_{max} - U_0) \tag{1}$$

where $U(t)$, U_0 and U_{max} are, respectively, the output voltage of the infrared detector as a function of time t, the minimum and the maximum of the thermogram.

The experimental (m_0 and m_{-1}) and theoretical (m_0^* and m_{-1}^*) partial time moments are written in a general way as follows, where $t_{0.1}$ and $t_{0.8}$ correspond to the times needed to the back face of the specimen to reach, respectively, 10 % and 80 % of the maximum amplitude of the thermogram:

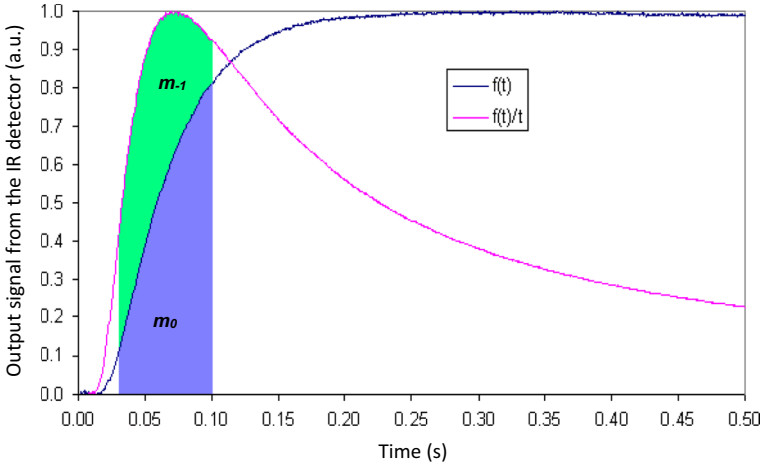

Fig. 2 Example of experimental thermogram

$$m_0 = \int_{t_{0.1}}^{t_{0.8}} f(t)dt \quad \text{and} \quad m_{-1} = \int_{t_{0.1}}^{t_{0.8}} f(t)/tdt \tag{2}$$

The theoretical and experimental partial time moments are linked by the two following relationships where e is the specimen thickness:

$$m_0 = m_0^* \cdot e^2/a \,\text{and}\, m_{(-1)} = m_{(-1)}^* \tag{3}$$

A relation between the theoretical moments m_0^* andm_{-1}^*, named identification function F, is established by a polynomial fit of couples of values (m_0^*,m_{-1}^*) calculated from thermograms obtained for various values of Bi using the analytical model. The coefficients b_i depend on the geometrical ratio R/e of the specimen (where R is the radius of the specimen).

$$m_0^* = F(m_{-1}^*) = \sum_{i=0}^{n} b_i \cdot (m_{-1})^i \tag{4}$$

Equation 5 gives as example the identification function F determined by LNE in the case of a 3 mm thick specimen with a diameter of 10 mm.

$$F\left(m_{-1}\right) = -0.06767 \cdot m_{-1} + 0.502198 \cdot m_{-1}^2 - 0.172615 \cdot m_{-1}^3 \tag{5}$$

The thermal diffusivity a is then given by the following relationship by combining Eqs. 3 and 4:

$$a = F(m_{-1}) \cdot e^2/m_0 \tag{6}$$

3 Assessment of Measurement Uncertainties

The analytical expression of the uncertainty associated to thermal diffusivity measurements performed with the new configuration of the laser flash apparatus of LNE is established in accordance with the ISO/BIPM Guide to the expression of uncertainty in measurement [13]. This uncertainty results from the combination of the standard uncertainties on the calculation of the partial time moments $u(m_0)$ and $u(m_{-1})$, on the thickness determination $u(e)$, on the establishment of the identification function $u(F)$, on the measurement process $u(\overline{a})$ and $u_{hyp}(a)$, and on the measurement of the specimen temperature $u_T(a)$.

The analytical expression of the variance $u^2(a)$ is determined by applying the propagation law of variances to the mathematical model given by Eq. 6, assuming that the partial time moments m_0 and m_{-1} are correlated together and are not dependent on the thickness e and on the identification function coefficients b_i. The coefficients b_i are assumed to be correlated together and not dependent on the thickness e.

$$\begin{aligned} u^2(a) =& c_{m_0}^2 \cdot u^2\left(m_0\right) + c_{m_{-1}}^2 \cdot u^2\left(m_{-1}\right) + 2 \cdot c_{m_0} \cdot c_{m_{-1}} \cdot u\left(m_0, m_{-1}\right) \\ &+ c_e^2 \cdot u^2(e) + c_F^2 \cdot u^2(F) + u^2\left(\overline{a}\right) + u_{hyp}^2(a) + u_T^2(a) \end{aligned} \tag{7}$$

with $c_e = 2 \cdot e \cdot \sum_{i=0}^{n} b_i \cdot m_{-1}^i / m_0 \quad c_F = e^2 / m_0$

$$c_{m_0} = -e^2 \cdot \sum_{i=0}^{n} b_i \cdot m_{-1}^i / m_0^2 \quad c_{m_{-1}} = e^2 \cdot \sum_{i=1}^{n} i \cdot b_i \cdot m_{-1}^{i-1} / m_0$$

The evaluations of the terms of Eq. 7 are summarized in the following sections. More detailed can be found in [11], in particular regarding the assessment of the variance $u^2\left(m_0\right)$ and $u^2\left(m_{-1}\right)$, and covariance $u\left(m_0, m_{-1}\right)$ of the partial time moments m_0 and m_{-1}.

3.1 Variances $u^2\left(m_0\right)$ and $u^2\left(m_{-1}\right)$ and Covariance $u\left(m_0, m_{-1}\right)$ of the Partial Time Moments

The uncertainty associated with the partial time moments m_0 and m_{-1} (calculated with Eq. 2) results from the combination of the uncertainties on the calculation of $f(t)$, on the measurement of the time t, on the determination of the limits of integration $t_{0.1}$ and $t_{0.8}$, and on the numerical integration method.

- The uncertainty on the normalized thermogram $f(t)$ (calculated with Eq. 1) results from the combination of the uncertainties on the measurement of the voltage $U(t)$ delivered by the IR detector, on the determination of the baseline U_0 and the maximum voltage U_{max}, and on the uncertainty due to the assumption of linearity of the voltage $U(t)$ coming from the IR detector with the temperature T of the rear face of the specimen.

The uncertainty on the measurement of the voltage $U(t)$ is due to the noise, and to the resolution and calibration of the detection chain, these three factors being considered as not correlated. The uncertainty due to the assumption of linearity is considered to be not dependent on the other uncertainty factors affecting the calculation of the normalized thermogram. As three IR detectors are used depending on the investigated temperature ranges, the assessment of this uncertainty factor has been done as a function of temperature for each detector, the sensitivity being different from one detector to another.

- The uncertainty associated with the measurement of the time t results from the combination of the uncertainties on acquisition time step Δt and on the determination of the initial time t_0. The duration and the temporal profile of the laser pulse are both taken into account in the determination of the initial time t_0 by shifting the origin of time by a value corresponding to the chronological centroid of the laser pulse, according to the correction method proposed by Azumi [24]. The uncertainty on the time t is actually equal to that on the initial time t_0, the uncertainty on Δt being negligible.

The term of covariance $u\left(m_0, m_{-1}\right)$ is attributable to the fact that the same normalized thermogram $f(t)$ is used for the calculation of the partial time moments m_0 and m_{-1}. It is considered that the only significant covariance between m_0 and m_{-1} is generated by the assumption of linearity of the detector response, the other uncertainty factors affecting the calculation of m_0 and m_{-1} being independent.

3.2 Variance of the Thickness $u^2(e)$

The thickness e_0 of the specimen is measured at room temperature RT (usually 23 °C) using a calibrated micrometre. At the test temperature $T > RT$, the thickness e of the specimen is equal to the thickness e_0 measured at RT corrected by the thermal expansion of the specimen between these two temperatures. The uncertainty associated to the determination of the thickness e results therefore from the combination of the uncertainties on the measurement of the thickness e_0 and on the calculation of the correction Δ_e due to thermal expansion performed according to Eq. 8.

$$\Delta_e = \alpha_l \cdot e_0 \cdot (T - RT) \tag{8}$$

- The uncertainty on the thickness e_0 results from the combination of the uncertainties due to the repeatability of measurements, and to the calibration and resolution of the micrometre, these three components being considered as independent.
- The uncertainty on the correction of the thickness results from the combination of the uncertainties on the determination of the mean coefficient of

linear thermal expansion α_l and on the measurement of the room temperature, the temperature of test and the specimen thickness e_0.

3.3 Variance of the Identification Function $u^2(F)$

The variance of the identification function F, which is established by a polynomial fit of couples of values (m_0^*, m_{-1}^*), is a combination of the variances of the coefficients b_i, the covariance between coefficients b_i and the residual variance of the regression due to the error of the model.

3.4 Variances Due to the Measurement Process $u^2(\overline{a})$ and $u^2_{hyp}(a)$

LNE determines the thermal diffusivity of a material at a given temperature by performing three successive measurements on the same specimen under repeatability conditions, the result being equal to the average of these measurements. The corresponding uncertainty factor $u(\overline{a})$, which is partially due to the operator effect for the selection of U_0 and U_{max}, is calculated from the repeatability of the three consecutive measurements.

Another uncertainty factor linked to the measurement process need to be assessed in addition.

All estimation techniques of thermal diffusivity based on the laser flash method assumed that the experimental conditions during the measurements are strictly identical to the hypotheses used to establish the theoretical model (cf. Sect. 2.2): Spatial uniformity of the energy deposited by the laser beam on the specimen front face, duration of the pulse negligible compared to the rear face temperature rise time, heat losses characterized by a uniform heat exchange coefficient.

The variance $u^2_{hyp}(a)$ due to the use of the function F for experimental conditions different from the assumptions for which it was determined, has been estimated by modelling the heat transfer in 3 mm thick specimens. This has been performed for different initial and boundary conditions, by changing the laser pulse duration, the spatial profil (*e.g.,* uniform or Gaussian) and diameter of the laser beam, the distribution of the heat-exchange coefficients on the specimen faces, and the diameter of the area sighted by the IR detector on the rear face of the specimen. The variance $u^2_{hyp}(a)$ is a combination of the standard uncertainties quantified for these four components, which are assumed to be not correlated.

3.5 Variance $u^2_T(a)$ on the Thermal Diffusivity Due to the Variance on the Test Temperature T

The specimen temperature T is measured either thanks to a thermocouple fixed on the sample holder for measurements performed in the resistive furnace (for temperature from 23 °C to 800 °C) or by using radiative thermometers for

measurements performed in the inductive furnace (from 700 °C to 3000 °C). The uncertainty associated to the measurement of T results from the uncertainty linked to the resolution and calibration of the temperature measuring chains, and the uncertainty due to the stability and the homogeneity of the furnaces temperature, these four uncertainty factors being considered independent.

As thermal diffusivity is a temperature-dependent physical property, the uncertainty on the temperature T has a contribution on the uncertainty associated to the thermal diffusivity measurement (even if temperature is not a parameter directly used in the determination of thermal diffusivity) via the relationship $a = G(T)$ giving the variation of thermal diffusivity *versus* temperature. The variance on the thermal diffusivity due to the variance on the test temperature T is expressed by Eq. 9, the polynomial relationship $a = G(T)$ being determined for each tested material from the experimental results obtained in the investigated temperature range.

$$u_T^2(a) = (\partial G(T)/\partial T)^2 \cdot u^2(T)$$

4 Application to the Study of Three Refractory Materials

The thermal diffusivity of three solid homogeneous refractory materials (pure molybdenum 99.9 % and tungsten 99.95 %, and isotropic graphite IG210 from Toyo Tanso) has been measured with the new configuration of the LFA of LNE (cf. Section 2), and the associated uncertainties have been assessed according to the method described in the Sect. 3. These materials have been selected due to their high melting point (2620 °C for the molybdenum and 3420 °C for the tungsten) or high sublimation temperature (more than 3650 °C for the graphite). The measurements have been performed from 23 °C to 2200 °C in case of molybdenum, up to 2400 °C for the tungsten and up to 3000 °C for the isotropic graphite.

The linear thermal expansion coefficient of the three studied materials was measured beforehand under inert atmosphere from 23 °C to 2000 °C, during three successive cycles with heating and cooling rates of 5 K·min^{-1}, with horizontally operating differential push rod dilatometer. The mean linear thermal expansion coefficient α_l between T_0= 23 °C and T is given by Eq. 10, where ΔL is the expansion measured between T_0 and T, and L_{T_0} is the length of the specimen at T_0. The data obtained are used for the measurements of thermal diffusivity at high temperature, in order to calculate the corrections on the specimen thickness due to thermal expansion.

$$\alpha_l = \frac{1}{T - T_0} \cdot \frac{\Delta L}{L_{T_0}} \tag{10}$$

The mean linear thermal expansion coefficients measured for the three materials by LNE are presented in Table 1 as a function of temperature. These values correspond to the average of the data obtained for the second and the third cycles. These materials exhibit indeed thermal expansion hysteresis for the first thermal cycle which could be explained by the relaxation of the residual stresses caused by the preparation (*e.g.,* machining) of the specimens.

Table 1 Mean thermal expansion coefficients of the isotropic graphite, tungsten and molybdenum

Mean thermal expansion coefficient (10^{-6} K^{-1})					
Temperature (°C)	Isotropic graphite	Tungsten		Molybdenum	
		LNE	[25, 26]	LNE	[27]
23	–	–	–	–	–
50	4.05	4.45	4.45	5.06	–
100	4.16	4.50	4.49	5.23	–
150	4.27	4.55	4.53	5.35	–
200	4.37	4.59	4.56	5.41	–
250	4.48	4.63	4.58	5.45	–
300	4.58	4.66	4.61	5.49	–
400	4.77	4.72	4.65	5.54	–
600	5.09	4.81	4.73	5.67	–
800	5.34	4.89	4.81	5.79	–
1000	5.51	4.98	4.89	5.94	–
1200	5.65	5.08	4.97	6.15	6.20
1400	5.78	5.20	5.07	6.40	6.40
1600	5.96	5.34	5.17	6.65	6.64
1800	6.21	5.52	5.29	7.07	6.90
2000	6.56	5.75	5.42	7.45	7.21

The maximum operating temperature of the dilatometer being 2000 °C, the mean coefficient of thermal expansion measured between 23 °C and 2000 °C is used to correct the thickness specimens for thermal diffusivity measurements performed above 2000 °C. The expanded uncertainty (coverage factor $k=2$) on thermal expansion coefficients of isotropic graphite, tungsten and molybdenum is estimated to be 10 %. The results are in good agreement with data obtained by absolute measurement methods based on interferometric techniques [25–27], the difference between LNE's results and published values being within the expanded uncertainty estimated by LNE.

Tables 2, 3, and 4 present the thermal diffusivity values obtained by LNE (for 3 mm thick specimens), respectively, for isotropic graphite IG210, tungsten and molybdenum as a function of temperature, as well as the associated expanded uncertainties ($k=2$). These thermal diffusivity values correspond to the average of three measurements repeated at each temperature level. The data in normal font refer to raw values of thermal diffusivity while the data in italic are corrected values that take into account the thermal expansion (given in Table 1) of the tested materials. Figures 3, 4, and 5 plot the corrected values of thermal diffusivity (without uncertainty bars for more readability) obtained for the three materials *versus* temperature.

Tables 5, 6, and 7 give three examples of uncertainty budget evaluated in the case of the measurement of thermal diffusivity of the isotropic graphite IG210 at 1000 °C, 2000 °C and 3000 °C, with detail of the different uncertainty components described in Sect. 3.

Table 2 Thermal diffusivity of isotropic graphite IG210 and associated uncertainty

Temperature (°C)	Thermal diffusivity (10^{-6} m^2·s^{-1})		Expanded Uncertainty ($k=2$)
	Raw data	Corrected value	(%)
23	87.91	*87.91*	3.2
50	78.38	*78.40*	3.2
100	64.83	*64.87*	3.1
149	55.22	*55.28*	3.1
199	47.33	*47.40*	3.1
249	41.42	*41.50*	3.0
300	36.88	*36.97*	3.0
400	30.05	*30.16*	3.0
601	22.35	*22.48*	3.0
806	18.27	*18.42*	3.1
1001	15.60	*15.77*	3.1
1198	13.71	*13.89*	3.3
1400	12.27	*12.47*	3.4
1601	11.18	*11.39*	3.7
1799	10.31	*10.54*	3.7
2001	9.54	*9.79*	3.8
2201	8.98	*9.24*	4.0
2398	8.46	*8.73*	4.2
2600	8.08	*8.36*	4.3
2796	7.77	*8.06*	4.4
2985	7.33	*7.62*	4.7

The relative expanded uncertainty $u(a)$ associated to thermal diffusivity measurements performed by the laser flash method, which corresponds to two standard deviations ($k=2$), is estimated to be between 3 % and 5 % for the three materials in the temperature range from 23 °C to 3000 °C.

It is maximal at the ends of the temperature range investigated here (*cf.* Tables 2, 3, and 4) and reaches a minimum between 300 °C and 600 °C. This is mainly due to the uncertainty components on the measurement of the IR detectors output voltage which vary in opposite ways when the temperature increases. The uncertainty due to the assumption of linearity of this voltage with the temperature, which is a preponderant component of the uncertainty $u\left(m_{-1}\right)$ at low temperature, decreases with increasing temperature until becoming negligible at 1400 °C. Conversely, signal to noise ratio which decreases when the temperature increases leads to a higher uncertainty on the determination the partial time moments m_0 and m_{-1} and to a worse repeatability of the three successive measurements at high temperature.

The Tables 5, 6, and 7 show that the main uncertainty components on thermal diffusivity measurement are those related to the calculation of the partial time moment m_{-1} and to the hypotheses used to establish the theoretical model. The contribution

Table 3 Thermal diffusivity of tungsten and associated uncertainty

Temperature (°C)	Thermal diffusivity (10^{-6} $m^2 \cdot s^{-1}$)		Expanded uncertainty ($k=2$)
	Raw data	Corrected value	(%)
23	68.61	*68.61*	3.5
51	65.65	*65.67*	3.5
100	62.72	*62.76*	3.4
149	59.92	*59.99*	3.4
199	57.44	*57.53*	3.4
250	54.88	*55.00*	3.3
301	52.55	*52.69*	3.2
401	49.12	*49.30*	3.2
601	44.12	*44.37*	3.3
802	40.63	*40.94*	3.5
991	38.18	*38.55*	3.7
1197	36.53	*36.97*	3.7
1397	34.74	*35.24*	3.8
1598	32.70	*33.25*	3.9
1799	30.90	*31.51*	4.0
1996	28.86	*29.52*	4.2
2195	26.87	*27.55*	4.6
2402	25.28	*25.98*	5.0

of the first one increases when temperature goes from 1000 °C to 3000 °C (cf. above explanations) while the relative weight of the second one in the uncertainty budgets decreases. This uncertainty associated with the theoretical assumptions is equal to about 1 % of the thermal diffusivity whatever the temperature and the material.

The relative contribution of the uncertainty due to test temperature measurement is relatively low up to 800 °C (less than 2 % of the total variance) when performing the thermal diffusivity measurements in the resistive furnace. It is between 3.2 % and 7.1 % if the measurements are performed from 1000 °C to 3000 °C with the inductive furnace. The standard uncertainty ($k=1$) associated with the measurement of the test temperature increases strongly from about 1 °C at 800 °C (with the resistive furnace) to 5.4 °C at 1000 °C and more than 15 °C at 3000 °C (with the inductive furnace), due to the uncertainties associated with the homogeneity and calibration of the inductive furnace, despite the *in situ* calibration procedure applied. Although the uncertainty in measuring the specimen temperature increases with temperature, its relative contribution remains less or equal to 7.1 % (cf. Tables 5, 6, 7) for all specimens in the whole temperature range, owing to weak temperature dependence of thermal diffusivity at elevated temperatures. The shape of the curve presented in Fig. 3 confirms that the thermal diffusivity of the isotropic graphite IG210 is less sensitive to temperature when the temperature increases (this behaviour is similar for tungsten and molybdenum).

Table 4 Thermal diffusivity of molybdenum and associated uncertainty

Temperature (°C)	Thermal diffusivity (10^{-6} $m^2 \cdot s^{-1}$)		Expanded uncertainty ($k=2$)
	Raw data	Corrected value	(%)
23	55.22	*55.22*	3.5
50	53.87	*53.88*	3.5
101	51.55	*51.59*	3.4
151	49.37	*49.44*	3.4
201	47.74	*47.83*	3.4
251	46.40	*46.52*	3.3
301	45.19	*45.33*	3.2
402	42.89	*43.07*	3.2
600	39.74	*40.00*	3.3
800	36.97	*37.30*	3.5
1000	34.55	*34.95*	3.7
1205	32.15	*32.62*	3.7
1400	29.29	*29.81*	3.8
1599	26.65	*27.21*	3.9
1799	24.29	*24.90*	4.0
1999	22.34	*23.00*	4.2
2201	20.12	*20.78*	4.7

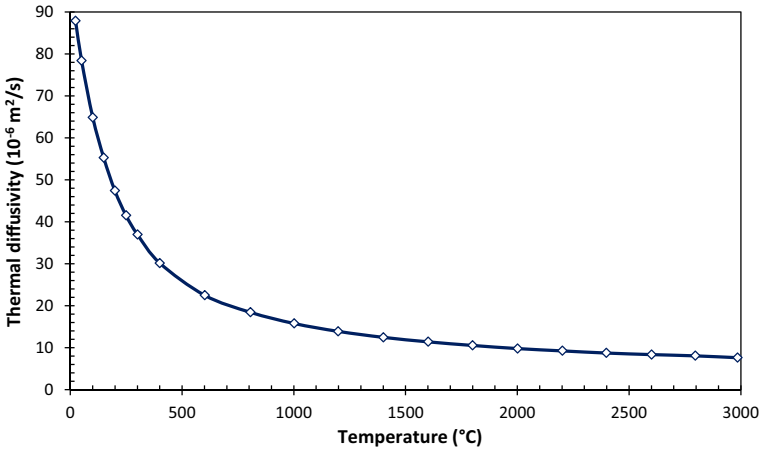

Fig. 3 Thermal diffusivity of the isotropic graphite IG210 measured by LNE from 23 °C to 3000 °C

As the thermal expansion of materials is here taken into account when determining the thickness of the specimen for diffusivity measurements carried out above 23 °C, then the associated uncertainty term has a relative contribution limited to about 1 % of the overall variance whatever the temperature and material. If the thermal expansion

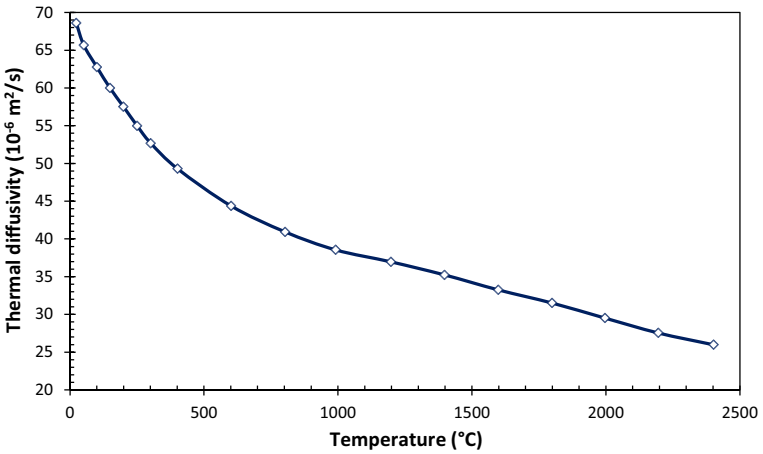

Fig. 4 Thermal diffusivity of the tungsten measured by LNE from 23 °C to 2400 °C

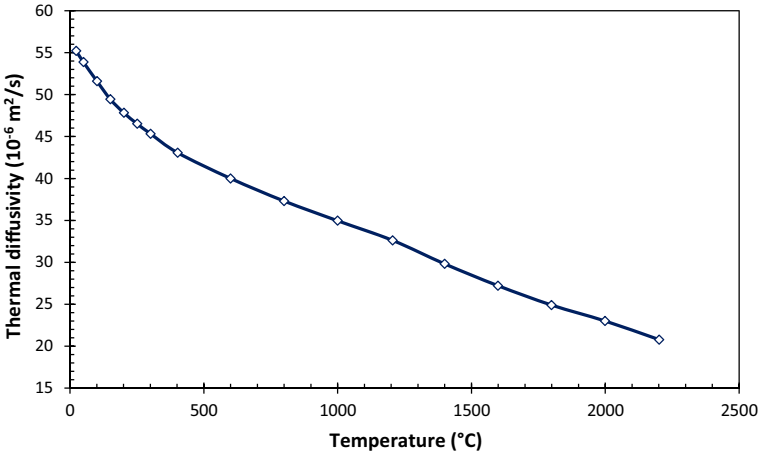

Fig. 5 Thermal diffusivity of the molybdenum measured by LNE from 23 °C to 2200 °C

of the specimen is not considered, then the thickness used in the calculation of the thermal diffusivity for all test temperatures is the one measured at room temperature. This results in an underestimation of the measured thermal diffusivity values which can reach here up to 2.7 %, 3.2 % and 3.8 %, respectively, in the case of tungsten at

Table 5 Uncertainty budget associated with thermal diffusivity value measured at 1000 °C

Uncertainty component	Value	Standard uncertainty ($k=1$) or covariance	Sensitivity coefficient	Contribution[a]
X_i	x_i	$u(x_i)$ or $u(x_i,x_j)$	$\partial a / \partial X_i$	(%)
Partial time moment m_{-1}	0.4944	1.86×10^{-3}	6.94×10^{-5} m^2·s^{-1}	27.8
Partial time moment m_0	0.0396 s	1.47×10^{-4} s	-3.97×10^{-4} m^2·s^{-2}	5.7
Covariance factor $u(m_0, m_{-1})$	0	2.77×10^{-9} s	-5.51×10^{-8} m^4·s^{-3}	−0.3
Thickness e	3.013×10^{-3} m	2.34×10^{-6} m	1.04×10^{-2} m·s^{-1}	1.0
Identification function F	0.06844	2.24×10^{-4}	2.30×10^{-4} m^2·s^{-1}	4.4
Theoretical assumptions	0	1.78×10^{-7} m^2·s^{-1}	1	52.9
Average of 3 measurements	15.77×10^{-6} m^2·s^{-1}	4.04×10^{-8} m^2·s^{-1}	1	2.7
Specimen temperature T	1001 °C	5.40 °C	1.10×10^{-8} m^2·s^{-1}·°C^{-1}	5.8
Thermal diffusivity a	Standard uncertainty		Expanded uncertainty ($k=2$)	
15.70×10^{-6} m^2·s^{-1}	2.45×10^{-7}m^2·s^{-1}		4.91×10^{-7}m^2·s^{-1}	3.1%

[a]The values expressed in % correspond to the contributions of each uncertainty component in terms of variance with respect to the total variance on the thermal diffusivity *a*

Table 6 Uncertainty budget associated with thermal diffusivity value measured at 2000 °C

Uncertainty component	Value	Standard uncertainty ($k=1$) or covariance	Sensitivity coefficient	Contribution
X_i	x_i	$u(x_i)$ or $u(x_i,x_j)$	$\partial a / \partial X_i$	(%)
Partial time moment m_{-1}	0.4595	2.59×10^{-3}	4.88×10^{-5} m^2·s^{-1}	44.8
Partial time moment m_0	0.0537 s	2.44×10^{-4} s	-1.86×10^{-4} m^2·s^{-2}	5.7
Covariance factor $u(m_0, m_{-1})$	0	5.30×10^{-9} s	-1.82×10^{-8} m^4·s^{-3}	−0.3
Thickness e	3.036×10^{-3} m	2.94×10^{-6} m	6.58×10^{-3} m·s^{-1}	1.1
Identification function F	0.05819	2.25×10^{-4}	1.72×10^{-4} m^2·s^{-1}	4.2
Theoretical assumptions	0	1.15×10^{-7} m^2·s^{-1}	1	37.0
Average of 3 measurements	9.79×10^{-6} m^2·s^{-1}	3.87×10^{-8} m^2·s^{-1}	1	4.2
Specimen temperature T	2001 °C	10.1 °C	3.35×10^{-9} m^2·s^{-1}·°C^{-1}	3.2
Thermal diffusivity a	Standard uncertainty		Expanded uncertainty ($k=2$)	
9.99×10^{-6} m^2·s^{-1}	1.89×10^{-7}m^2·s^{-1}		3.78×10^{-7}m^2·s^{-1}	3.8%

Table 7 Uncertainty budget associated with thermal diffusivity value measured at 3000 °C

Uncertainty component	Value	Standard uncertainty ($k=1$) or covariance	Sensitivity coefficient	Contribution
X_i	x_i	$u(x_i)$ *or* $u(x_i,x_j)$	$\partial a / \partial X_i$	*(%)*
Partial time moment m_{-1}	0.3975	3.05×10^{-3}	4.61×10^{-5} $m^2{\cdot}s^{-1}$	61.2
Partial time moment m_0	0.0506 s	3.40×10^{-4} s	-1.52×10^{-4} $m^2{\cdot}s^{-2}$	8.3
Covariance factor $u(m_0, m_{-1})$	0	2.43×10^{-9} s	-1.40×10^{-8} $m^4{\cdot}s^{-3}$	−0.1
Thickness e	3.055×10^{-3} m	3.67×10^{-6} m	5.02×10^{-3} $m{\cdot}s^{-1}$	1.1
Identification function F	0.04161	2.24×10^{-4}	1.84×10^{-4} $m^2{\cdot}s^{-1}$	5.3
Theoretical assumptions	0	5.81×10^{-8} $m^2{\cdot}s^{-1}$	1	10.5
Average of 3 measurements	7.62×10^{-6} $m^2{\cdot}s^{-1}$	4.62×10^{-8} $m^2{\cdot}s^{-1}$	1	6.6
Specimen temperature T	2985 °C	15.2 °C	3.14×10^{-9} $m^2{\cdot}s^{-1}{\cdot}°C^{-1}$	7.1
Thermal diffusivity a	Standard uncertainty		Expanded uncertainty ($k=2$)	
7.67×10^{-6} $m^2{\cdot}s^{-1}$	$1.79\times10^{-7}m^2{\cdot}s^{-1}$		$3.58\times10^{-7}m^2{\cdot}s^{-1}$	4.7%

2402 °C, molybdenum at 2201 °C and graphite at 2985 °C (cf. Tables 2, 3, 4). The order of magnitude of these errors being the same as that of the expanded uncertainty for the temperatures above 1000 °C, it is therefore essential to apply a thermal expansion correction in the determination of the specimen thickness used for high temperature thermal diffusivity measurements by the laser flash method.

5 Conclusions

The assessment of the uncertainties associated with high temperature thermal diffusivity measurements by the laser flash method is described in detail in this paper for the first time. These uncertainties were calculated taking into account the different sources of uncertainty, such as the measurement method, the calibration and measurement means, the environmental conditions, etc. The influence parameters were identified and quantified and the analytical expression of measurement uncertainty was established. Thermal diffusivity values measured on isotropic graphite, tungsten and molybdenum in the temperature range from 23 °C to 3000 °C, with a laser flash apparatus adapted at LNE, are presented with their corresponding expanded uncertainty ($k=2$). The expanded relative uncertainty associated with the thermal diffusivity determination is estimated to be between 3 % and 5 % for the three refractory materials, if the thermal expansion of the tested specimens is corrected. Uncertainty budgets presented for the isotropic graphite at 1000 °C, 2000 °C and 3000 °C show

that the main uncertainty components are those related to the analysis of the experimental curve, in particular due to the noise on the IR signal, and to some bias in the application of the laser flash method itself where the initial and boundary conditions are not exactly the same for the theoretical model and for the experiment.

Acknowledgments This project 17IND11 Hi-TRACE has received funding from the EMPIR programme co-financed by the Participating States and from the European Union's Horizon 2020 research and innovation programme.

References

1. Y. Katoh, L. Snead, J. Nucl. Mater. **526**, 151849 (2019). https://doi.org/10.1016/j.jnucmat.2019.151849
2. Wings in Orbit: Scientific and Engineering Legacies of the Space Shuttle, 1971–2010, chap. Thermal protection systems, 182–199, NASA, ISBN 978-0160868467 (2011)
3. L. Hallstadius, S. Johnson, E. Lahoda, Prog Nucl Energy **57**, 71 (2012). https://doi.org/10.1016/j.pnucene.2011.10.008
4. Z. Duan, H. Yang, Y. Satoh, K. Murakami, S. Kano, Z. Zhao, J. Shen, H. Abe, Nucl. Eng. Des. **316**, 131 (2017). https://doi.org/10.1016/j.nucengdes.2017.02.031
5. R. Monti, M. De Stefano Fumo, R. Savino, J. Thermophys. Heat Transf. **20**, 500 (2006). https://doi.org/10.2514/1.17947
6. E. Boulier, G. Pinaud, P. Bugnon, Thermal issues related to Exomars EDLS performance, in *Proceeding of 28th European Space Thermal Analysis Workshop*, ESA/ESTEC, Noordwijk, The Netherlands, Oct. 14th–15th 2014, 117–126, European Space Agency - ISSN 1022–6656 (2014)
7. F. Buffenoir, T. Pichon, R. Barreteau, Thermal protection system post-flight preliminary analysis, in *7th European Conference for Aeronautics and Space Science*, Milan (2017). https://doi.org/10.13009/EUCASS2017-330
8. K. Boboridis, B. Hay, ATW-Int. J. Nucl. Power **65**, 140 (2020)
9. T. Baba, A. Ono, Meas. Sci. Technol. **12**, 2046 (2001). https://doi.org/10.1088/0957-0233/12/12/304
10. L. Vozár, W. Hohenauer, Int. J. Thermophys. **26**, 1899 (2005). https://doi.org/10.1007/s10765-005-8604-5
11. B. Hay, J.-R. Filtz, J. Hameury, L. Rongione, Int. J. Thermophys. **26**, 1883 (2005). https://doi.org/10.1007/s10765-005-8603-6
12. F.L. Migliorini, E.H.C. Silva, P.A. Grossi, R. A.N. Ferreira, D.M. Camarano, Calculated uncertainty of the thermal diffusivity measurement based on flash laser method, in *XIX IMEKO World Congress, Fundamental and Applied Metrology*, September 6–11, 2009, Lisbon, Portugal
13. JCGM 100:2008 (GUM 1995 with minor corrections) - Evaluation of measurement data - Guide to the expression of uncertainty in measurement (2008)
14. I. Pencea, I. Plotog, M. Branzei, A. Bibis, P. Svasta, *Proceedings of the 36th International Spring Seminar on Electronics Technology,* 195 (2013). https://doi.org/10.1109/ISSE.2013.6648241
15. A. Allard, N. Fischer, G. Ebrard, B. Hay, P. Harris, L. Wright, D. Rochais, J. Mattout, Metrologia **53**, S1–S9 (2016). https://doi.org/10.1088/0026-1394/53/1/S1
16. A. Lunev, R. Heymer, Rev. Sci. Instrum. **91**, 064902 (2020). https://doi.org/10.1063/1.5132786
17. B. Hay, J. Hameury, J.-R. Filtz, F. Haloua, R. Morice, High Temp-High Press **39**, 181 (2010)
18. W.J. Parker, R.J. Jenkins, G.L. Abbott, J. Appl. Phys. **32**, 1679 (1961). https://doi.org/10.1063/1.1728417

19. A. Degiovanni, M. Laurent, Rev. Phys. Appl. **21**, 229 (1986). https://doi.org/10.1051/rphysap:01986002103022900
20. B. Hay, L. Rongione, J.-R. Filtz, J. Hameury, High Temp-High Press **37**, 13 (2008)
21. M. Akoshima, B. Hay, J. Zhang, L. Chapman, T. Baba, The international pilot comparison on thermal diffusivity measurement using the laser flash method, Thermal Conductivity **30**, 367, ISBN 978-1-60595-015-0 (2010)
22. M. Akoshima, B. Hay, J. Zhang, L. Chapman, T. Baba, Int. J. Thermophys. **34**, 763 (2013). https://doi.org/10.1007/s10765-012-1209-x
23. G. Failleau, N. Fleurence, O. Beaumont, R. Razouk, J. Hameury, B. Hay, High Temp-High Press **50**, 149 (2021). https://doi.org/10.32908/hthp.v50.1013
24. T. Azumi, Y. Takahashi, Rev. Sci. Instrum. **52**, 1411 (1981). https://doi.org/10.1063/1.1136793
25. R. Kirby, T. Hahn, Certificate of Standard Reference Material 737. Tungsten - thermal expansion, National Bureau of Standards, Washington (1976)
26. A.P. Miiller, A. Cezairliyan, Int. J. Thermophys. **11**, 619 (1990). https://doi.org/10.1007/BF01184332
27. A.P. Miiller, A. Cezairliyan, Int. J. Thermophys. **6**, 695 (1985). https://doi.org/10.1007/BF00500340